Paper accepted for presentation at 2009 IEEE Bucharest Power Tech Conference, June 28th - July 2nd, Bucharest, Romania

Integration of Hydrogen Generator into Wind Farm Interconnected HVDC System

S.M. Muyeen, *Member*, *IEEE,* R. Takahashi, *Member*, *IEEE,* T. Murata, and J. Tamura, *Senior Member*, *IEEE*

***Abstract*— This paper presents the integration of hydrogen generation scheme into wind farm interconnected high-voltage DC (HVDC) system. The offshore wind farm composed of variable speed wind turbines driving permanent magnet synchronous generators and HVDC transmission system based on three-level (3L) neutral point clamped (NPC) voltage source converter (VSC) for the interconnection between offshore wind farm and onshore grid connection point are considered in this study. Suitable topology for hydrogen generation system composed of rectifier and chopper controlled electrolyzer unit is considered in this study to generate hydrogen using electrical power from offshore wind farm. Real wind speed date is used in the simulation study to obtain realistic response. Both dynamic and transient analyses of the proposed system are carried out using laboratory standard power system software package, PSCAD/EMTDC.**

***Index Terms*— electrolyzer, high voltage DC (HVDC), permanent magnet synchronous generator (PMSG), transient stability, variable speed wind turbine (VSWT), and voltage source converter (VSC).**

I. Introduction

RECENTLY generation of electricity using wind power has received much interest and considerable attention all over the world. According to EWEA reporting, 12% of the world's electricity is expected to be generated from wind power by 2020 [1]. Besides the onshore trend, offshore wind farms have also been continuing its growth rapidly. Some leading countries in wind energy arena are focusing more on offshore technology. The main reasons for adopting offshore are lack of the suitable onshore sites and much better wind conditions of offshore sites (wind is much stronger and more constant). Only by 2007, the industry had developed 25 projects with a total capacity of around 1,100 MW in five countries in Europe [2], many of which are large-scale and fully commercial.

Offshore wind farms are located, in general, 100 km or more far from the onshore grid connection point. It is a great challenge for both wind farm developer and transmission system operator (TSO) to transmit hundreds of MW offshore wind power over such a long distance. This paper focuses on high-voltage DC (HVDC) system for offshore wind farm interconnection with the onshore grid. Two types of HVDC transmission topologies, i.e., HVDC with voltage source converter using IGBTs (VSC-HVDC) and line-commutated converter HVDC (LCC-HVDC) are used nowadays for offshore wind farm connectivity [3-8]. However, in this study, VSC based HVDC transmission system is considered for offshore wind farm connectivity to the grid.

The use of VSC-HVDC for offshore wind farm connectivity has been reported already in some literatures [5-8]. In [5, 6], the wind farm considered are composed of fixed speed induction generators. In [7], synchronous generators are used in the offshore wind farm. Doubly fed induction generator (DFIG) is chosen as wind generator for offshore wind farm in [8]. However, PMSG is becoming very popular nowadays as variable speed wind generator. In PMSG, the excitation is provided by permanent magnets instead of field winding. Permanent magnet machines are characterized as having large air gaps, which reduce flux linkage even in machines with multi magnetic poles [9, 10]. As a result, low rotational speed generators can be manufactured with relatively small sizes with respect to its power rating. Moreover, gearbox can be omitted due to low rotational speed in PMSG wind generation system, resulting in low cost. In a recent survey, gearbox is found to be the most critical component, since its downtime per failure is high in comparison to other components in a wind turbine generator system (WTGS) [11].

Therefore, in this study, PMSG is considered as the wind generator for offshore wind farm. Variable speed wind turbine (VSWT) driving PMSG is connected to the electrical network through a fully controlled frequency converter which consists of AC/DC generator side converter, DC-link, and DC/AC grid side inverter. In both offshore and onshore HVDC stations, three-level (3L) neutral point clamped (NPC) VSCs are used. Suitable control strategies are developed for both offshore and onshore VSC stations. Another salient feature of this study is the integration of hydrogen generator at onshore VSC station to generate hydrogen constantly, using some portion of electrical power supplied from offshore wind farm. Recently, hydrogen has received much attention as a solution to the future energy crisis since it can be produced, stored, and even used for the electric power generation through fuel cell, without emissions of green house gas [12]. The hydrogen generator used in this study is composed of rectifier, duty cycle controlled DC chopper, and electrolyzer unit. Real wind speed data measured

This work was supported by the Grant-in-Aid for JSPS Fellows from Japan Society for the Promotion of Science (JSPS).

Authors are with the Electrical and Electronic Engineering Department, Kitami Institute of Technology, 165 Koen-Cho, Kitami, Hokkaido, 090-8507, Japan (e-mail: muyeen@pullout.elec.kitami-it.ac.jp).

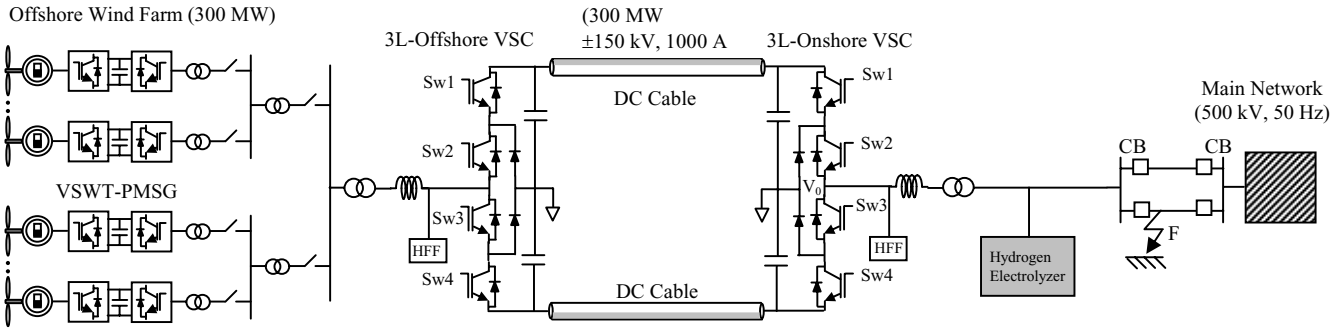

Fig. 1. Single line diagram of the proposed system

in Hokkaido Island, Japan, is used in the simulation analyses to obtain the realistic responses. Both dynamic and transient analyses of the proposed system composed of offshore wind farm,VSC-HVDC system, and hydrogen generator are carried out using PSCAD/EMTDC.

II. System Overview

The single line diagram of the proposed system composed of offshore wind farm, two 3L VSC-HVDC stations, two DC cross-linked polyethylene (XLPE) cables, and hydrogen generator is shown in Fig. 1. The offshore wind farm is composed of VSWTs driving PMSGs. The offshore wind farm power capacity is considered as 300 MW. However, to speed up the simulation aggregated model of wind farm is considered in the simulation, where several small size wind generators are represented with a large capacity wind generator.

The proposed system is connected to the main grid through transmission lines. Hence, the active power from the offshore wind farm is transmitted to the main grid via two DC XLPE cables. The cable model available in PSCAD software is used in the simulation. The ABB 150 kV XLPE cable parameters shown in the Appendix are used in this study. The cable length is considered as 100 km. A high-pass filter (HFF) is connected at both offshore and onshore VSC stations to absorb the well-defined harmonics for three-level converter/inverter systems. The individual component modeling is demonstrated below.

III. Modeling of Offshore Wind Farm

A. Wind Turbine Modeling

The mathematical relation for the mechanical power extraction from the wind can be expressed as follows [13]:

$$P_w = 0.5\rho\pi R^2 V_w^3 C_P(\lambda,\beta) \quad (1)$$

where, P_w is the extracted power from the wind, ρ is the air density [kg/m^3], R is the blade radius [m], V_w is the wind speed [m/s], and C_p is the power coefficient which is a function of both tip speed ratio, λ, and blade pitch angle, β [deg]. The wind turbine characteristics used in this study is shown in Fig. 2. The numerical expressions of it are available in [12].

The rotor speed is chosen as the control input for maximum power point tracking (MPPT) procedure as explained in [14]. If the reference maximum power, P_{max}, is greater than the rated power of PMSG, then the pitch controller used in [14] is considered to control the rotational speed. Therefore, output power will not exceed the rated power of the PMSG.

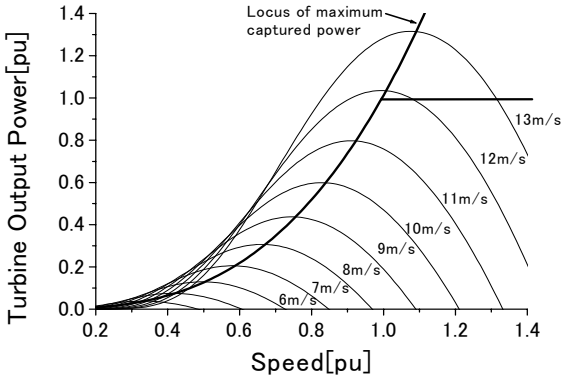

Fig. 2. Turbine characteristic with maximum power point tracking

B. Modeling of the frequency Converter of VSWT-PMSG

In this study, the direct drive VSWT-PMSG concept is adopted with the utilization of fully controlled frequency converter. The frequency converter consists of generator side AC/DC converter, DC link capacitor, and grid side DC/AC inverter. Each of converter/inverter is a standard 3-phase two-level unit, composed of six IGBTs and antiparallel diodes. The control strategy of the frequency converter considered in this study for VSWT-PMSG operation is the same that used in our previous study [14]. However, time average model is used in the simulation of frequency converter instead of the detailed switching model that used in [14] to speed up the simulation of large system. Thus, the DC-link circuit of the frequency converter is idealized as shown in Fig. 3 and expressed by eq.(2).

$$V_{dc} = \frac{1}{C}\int i\,dt \quad (2A)$$

$$i = i_c - i_i \quad (2B)$$

where, V_{dc} and C are frequency converter DC-link voltage, and DC-link capacitor values, respectively. i_c, i_i, and i are the currents of converter, inverter, and capacitor, respectively.

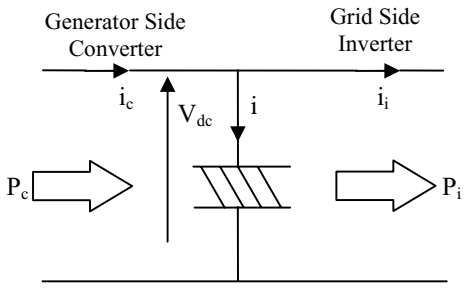

Fig. 3. DC-link circuit of the frequency converter

IV. Modeling of Offshore VSC Station

As the frequency converter of VSWT-PMSG can maintain constant voltage and frequency of the grid side, a simple control strategy based on modulation control is adopted for the control of offshore VSC station. The offshore VSC is controlled and operated as a voltage source with constant AC frequency and phase angle [8]. The Modulation index, M, control strategy is shown in Fig. 4. The modulated angle zero is applied to the PWM generator in phase A. The angles for phases B and C will be shifted by 120 and 240 degrees respectively. The insulated gate bi-polar transistor (IGBT) switching table for 3L NPC based offshore VSC station is shown in Table I. The gate pulses are generated with comparing the reference signals with double triangular wave. The switching frequency is chosen as 1050 Hz.

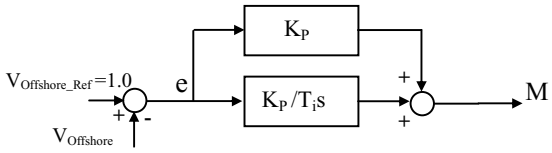

Fig. 4. Control block of offshore VSC station

TABLE I
THE SWITCHING TABLE

V_0	$+V_{dc}$	0	$-V_{dc}$
SW1	1	0	0
SW2	1	1	0
SW3	0	1	1
SW4	0	0	1

V. Modeling of Onshore VSC Station

Three-level onshore VSC control strategy is developed based on cascaded control as shown in Fig. 5. The reference signals are compared with double carrier wave signal to generate the switching signals for 3L NPC VSC according to the switching rule shown in Table I. The dq quantities and three-phase electrical quantities are related to each other by reference frame transformation. The angle of the transformation is detected from three phase voltages (v_a,v_b,v_c) at high voltage side of the grid side transformer by using phase lock loop (PLL). The d-axis current can control the DC voltage of the HVDC line. On the other hand, the q-axis current can control the reactive power of onshore station and hence the terminal voltage at high voltage side of the transformer can be kept constant at desired reference level set by transmission system operator (TSO).

VI. Modeling of Hydrogen Generator

The Faraday's law for electrolysis can be expressed briefly with the following equation.

$$\eta = \frac{It}{zF} \tag{3}$$

Where I is the current in Ampere, t is the time in sec, z is the valence number of ions of the substance (electrons transferred per ion), F is the Faraday Constant, and η is the amount of substance ("number of moles") produced.

According to the Faraday's Law of Electrolysis, it is possible to generate hydrogen gas by using electrolyzer (ELL). From eq.(3), it is clear that the amount of produced hydrogen depends on only the electrolyzer current. Therefore, the hydrogen generator can be simulated with the electrolyzer and the power
electronic devices that will provide constant current to the electrolyzer.

The schematic diagram of the hydrogen generator used in this study is shown in Fig. 6, which is composed of rectifier, DC chopper, and electrolyzer. The electrolyzer characteristic described in [12] is considered in this study. Electrolyzer power rating is considered 50 MW. In this analysis, the lumped model of electrolyzer is used in the simulation. The capacity of

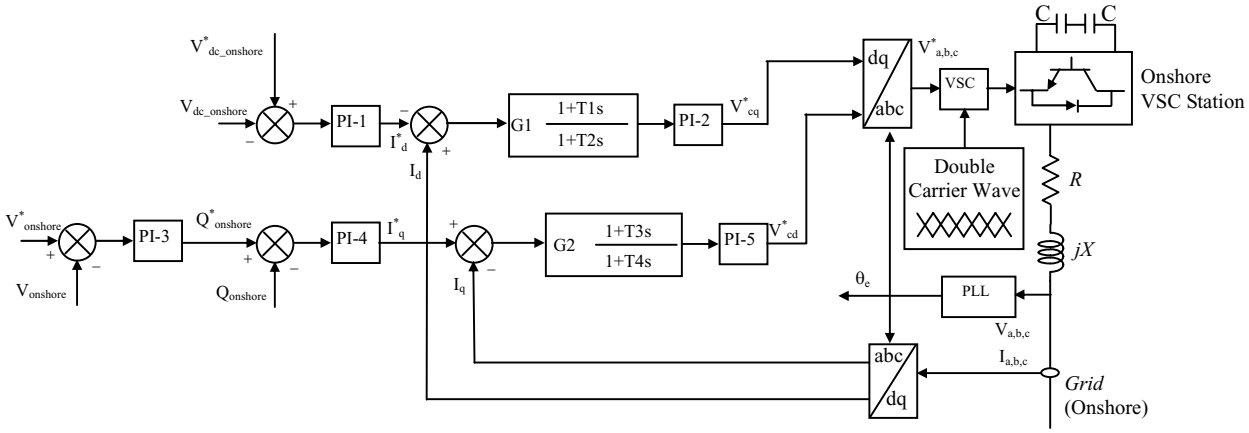

Fig. 5. Control block diagram of three-level PWM onshore VSC station

the individual electrolyzer cell is assumed to be 44.1 kW. One string consists of 42 cells. The lumped model consists of 27 strings working in parallel to ensure the sufficient electrolytic current. The parameters of the individual cell and lumped model of the electrolyzer are shown in Table II and Table III respectively.

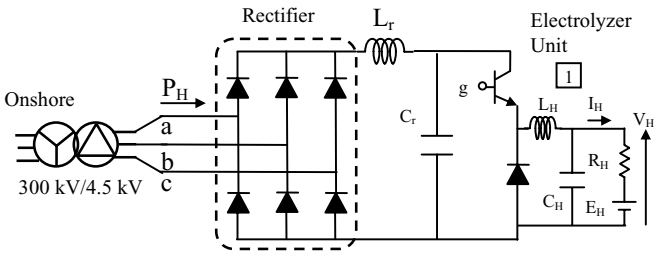

Fig. 6. Hydrogen electrolyzer

TABLE II
SPECIFICATIONS OF ONE ELECTROLYZER CELL

Rated power consumption	44.1[kW]
Rated voltage	107.5[V]
Hydrogen gas volume	7.5[Nm^3]/hr
Resistance	0.031[Ω]
DC source	94.8[V]

TABLE III
LUMPED MODEL PARAMETERS OF ELECTROLYZER

Inductance L_H	1.0[mH]
Resistance R_H	0.048[Ω]
DC source E_H	3.98[kV]

The hydrogen production is maintained constant at 50MW by controlling the DC chopper gate signal as shown in Fig. 7. The error signal between electrolyzer current and its reference is progressed through a PI controller and generates the chopper duty cycle. The duty cycle of the chopper is compared with the triangular carrier signal and generates the gate signal for IGBT device of DC chopper. The triangular carrier frequency is chosen 1000 Hz. The electrolyzer reference current is increased gradually by using a rate limiter as shown in Fig. 7 for soft switching operation of electrolyzer unit.

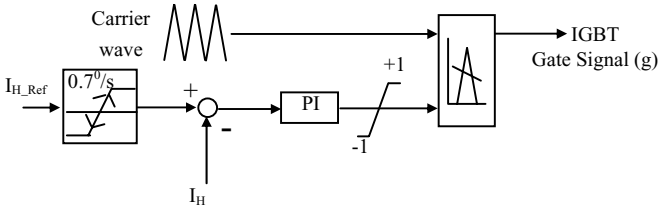

Fig. 7. Control block of electrolyzer DC chopper

VII. SIMULATION RESULTS

Both dynamic and transient characteristics are analyzed using the proposed system. The simulation time step is chosen as 0.00002 sec. The simulation time for dynamic and transient analyses are chosen as 600 sec and 10 sec, respectively.

A. Dynamic Characteristics Analysis

The real wind speed data used in the simulation are shown in Fig. 8, which was measured in Hokkaido Island, Japan. The responses of real power output from VSWT-PMSG, i.e., output of offshore wind farm and the rotor speed PMSG are shown in Figs. 9 and 10, respectively. Responses of real powers supplied

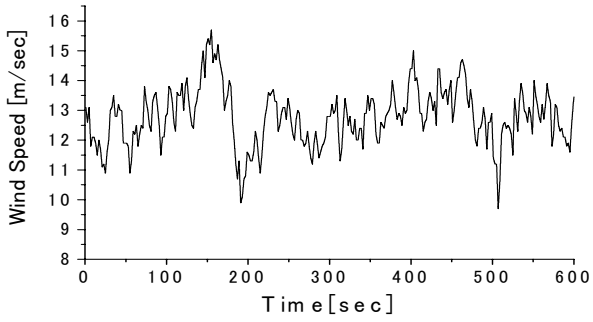

Fig. 8. Wind speed data

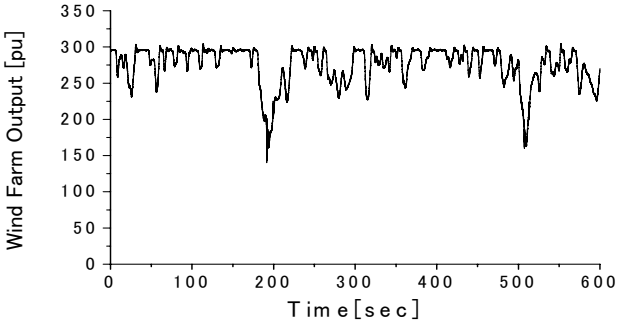

Fig. 9. Offshore wind farm real power

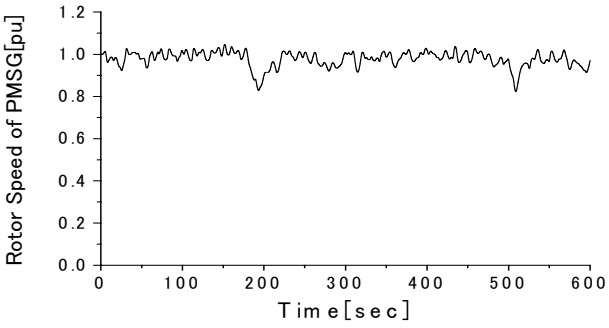

Fig. 10. Rotor speed of PMSG

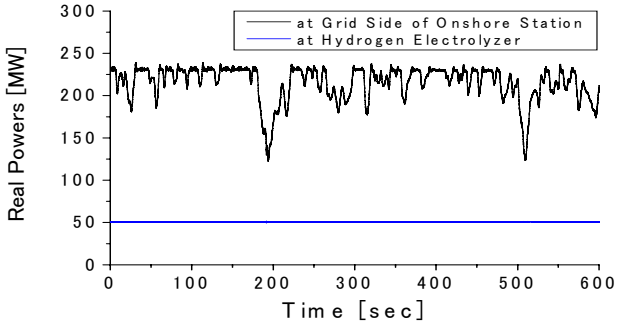

Fig. 11. Real powers supplied to the main network and hydrogen electrolyzer.

to the main network and electrolyzer are shown together in Fig. 11. The response of total hydrogen generation is shown in Fig. 12. The DC voltage responses of offshore and onshore VSC stations are shown in Figs. 13 and 14, respectively. Grid voltage at both onshore and offshore VSC stations are shown together in Fig. 15.

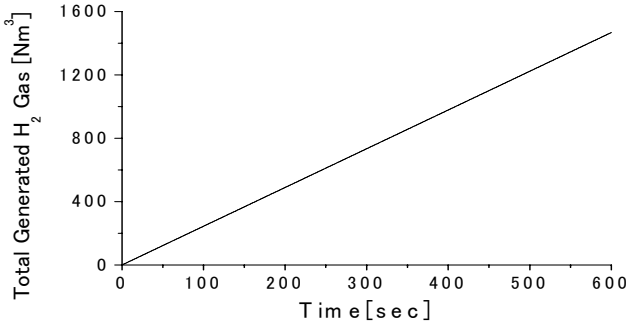

Fig. 12. Total generated hydrogen gas

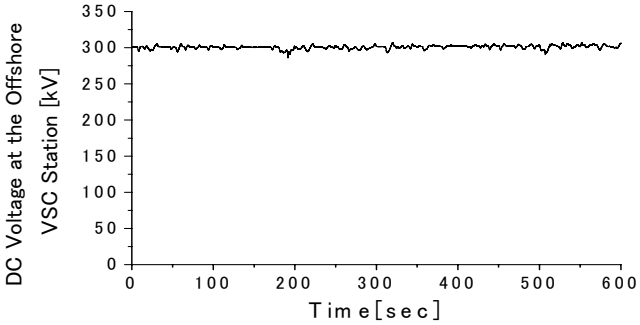

Fig. 13. DC voltage at the offshore VSC station

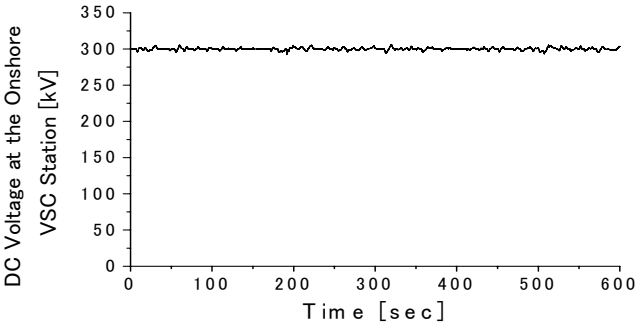

Fig. 14. DC voltage at the onshore VSC station

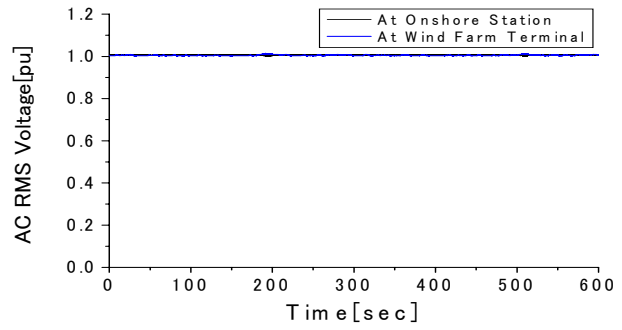

Fig. 15. Grid voltage at offshore and onshore VSC stations

B. *Transient Characteristics Analysis*

For transient stability analysis, the symmetrical severe three-line-to-ground fault (3LG) is considered as a network disturbance, which occurs at the grid side of the onshore VSC station (fault points F in Fig. 1). The fault occurs at 0.1 sec, the circuit breakers (CB) on the faulted lines are opened at 0.2 sec, and at 1.0 sec the circuit breakers are reclosed. In this analysis, it is assumed that wind speed is constant and equivalent to the rated speed for the offshore wind farm. This is because it may be considered that wind speed does not change dramatically during the short time interval of the simulation. When the onshore grid voltage goes lower than a certain value during network disturbance (in this study 0.85 pu), the wind farm power command signal is varied according to the grid voltage at the onshore VSC station. The responses of AC voltages at both VSC stations are shown together in Fig. 16. The real and reactive power responses at onshore side is shown in Fig. 17. The PMSG rotor becomes stable as shown in Fig. 18. The DC voltage at both offshore and onshore VSC stations are shown in Figs. 19 and 20, respectively. The DC voltages increase at the

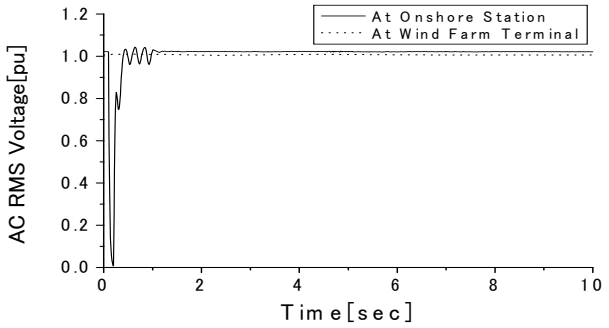

Fig. 16. AC-side voltages at offshore and onshore VSC stations (3LG)

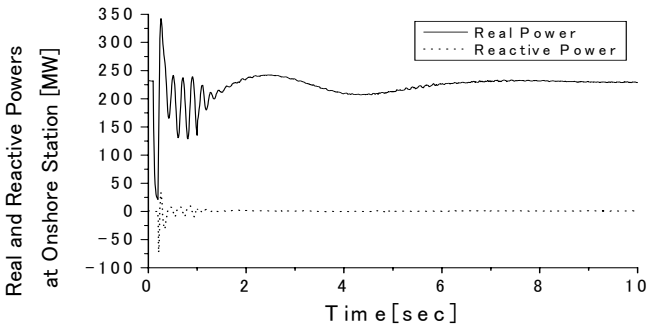

Fig. 17. Real and reactive powers at onshore VSC station (3LG)

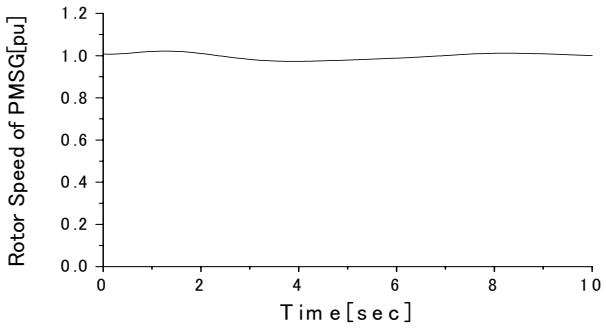

Fig. 18. Rotor speed of PMSG (3LG)

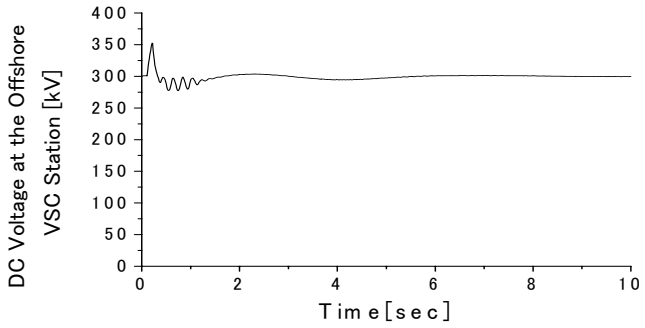

Fig. 19. DC voltage at the offshore VSC station (3LG)

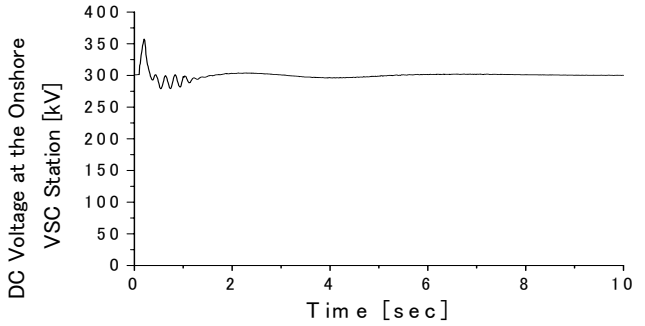

Fig. 20. DC voltage at the onshore VSC station (3LG)

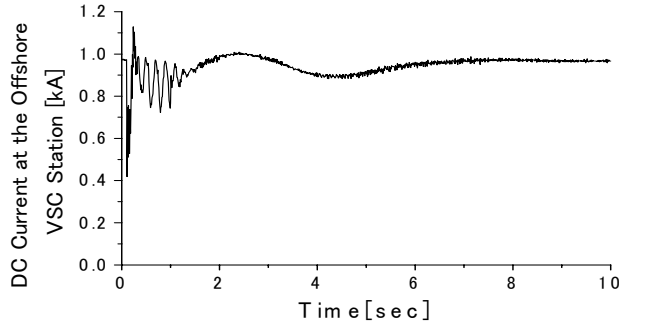

Fig. 21. DC current at the offshore VSC station (3LG)

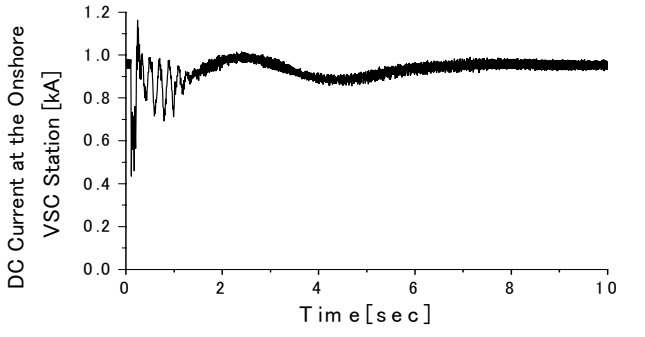

Fig. 22. DC current at the onshore VSC station (3LG)

beginning of the fault because the offshore wind farm continues to supply energy into the cable though the power transfer capability of the onshore VSC station decreases due to the short circuit fault. However, when the onshore grid voltage goes below 0.85 pu, the power transfer from offshore wind farm is reduced and dc voltages start to decrease. The responses of DC currents at both offshore and onshore VSC stations are shown in Figs. 21 and 22, respectively.

Simulation results clearly show that the proposed system can overcome severe 3LG fault under the developed control strategies.

VIII. Conclusions

In this paper, a new topology composed of offshore wind farm, 3L VSC-HVDC system, and electrolyzer unit has been presented. The offshore wind farm is composed of variable speed wind turbines driving Permanent magnet synchronous generators. Suitable control strategies for the 3L NPC based VSC-HVDC system and electrolyzer are discussed. Both dynamic and transient performances of the proposed system are analyzed by using simulation results, which validate the effectiveness of the developed control systems.

IX. Acknowledgment

The authors acknowledge contributions from Thomas Ackermann and Stephan Meier for providing some valuable technical data.

X. Appendix

The ABB 150 kV XLPE cable parameters are shown below [15].

Cable Parameters

Conductor Radius	0.0178 m
Insulator Outer radius	0.0370 m
Copper Resistivity	1.724e-8
Permittivity	2.3
Resistance at 20°C	0.0172 Ω/km

XI. References

[1] The European Wind Energy Association, EWEA Publications, 2005, "Wind Force 12- A Blueprint to Achieve 12% of the World's Electricity From Wind power by 2020," 2005, [Online], http://www.ewea.org/

[2] The European Wind Energy Association, "Delivering Offshore Wind Power in Europe: Pollicy Recommendations for Large-Scale Deployment of Offshore Wind Power in Europe by 2020," 2007.

[3] NM. Kirby, L. Xu, M. Luckett, and W. Siepman, "HVDC transmission for large offshore wind farms, IEE Power Engineering Journal; 3: 135–141, 2002.

[4] P. Cartwright, L. Xu, "The integration of large scale wind power generation into transmission networks using power electronics," CIGRE General Session, Paris, 2004 (CD-ROM).

[5] AK. Skytt, P. Holmberg, KE. Juhlin, "HVDC light for connection of wind farms," 2nd International Workshop on Transmission Networks for Offshore Wind Farms, 2001.

[6] KH. Sobrink, PL. Sorensen, P. Christensen, N. Sandersen, K. Eriksson, P. Holmberg,. "DC feeder for connection of a wind farm," CIGRE Symposium, 1999.

[7] W. Lu, BT. Ooi, "Optimal acquisition and aggregation of offshore wind power by multiterminal voltage-source HVDC," IEEE Transactions on Power Delivery, vol.18, No.1, pp.201–206, 2003.

[8] L. Xu, and B. R. Andersen, "Grid Connection of Large Offshore Wind Farms Using HVDC," Wind Energy, Vol.9, No.4, pp.371-382, 2006.

[9] Peter Vas, "Electrical machines and Drives- A Space Vector Theory Approach," Oxford University Press, New York, United States, 1992.

[10] T. J. E. Miller, "Brushless Permanent-Magnet and Reluctance Motor Drives," Oxford University Press, New York, United States, 1989.

[11] J. Ribrant and L. M. Bertling, "Survey of Failures in Wind Power Systems With Focus on Swedish Wind Power Plants During 1997-2005,"

IEEE Trans. on Energy Conversion, Vol. 22, No. 1, pp.167-173, March 2007.
[12] S. M. Muyeen, T. Murata, and J.Tamura, Stability Augmentation of a Grid-connected Wind Farm, United Kingdom, Springer, October 2008.
[13] S. Heier, Grid Integration of Wind Energy Conversion System, Chicester, UK, John Wiley & Sons Ltd., 1998.
[14] S. M. Muyeen, R. Takahashi, T.Murata, J.Tamura, and M. H. Ali, "Transient Stability Analysis of Permanent Magnet Variable Speed Synchronous Wind Generator," Proceedings of International Conference on Electrical Machines and Systems 2007 (ICEMS 2007), pp.288-293, Seoul, Korea, October 2007.
[15] XLPE Underground Cable Systems, ABB User's Guide, rev.3.

XII. BIOGRAPHY

S. M. Muyeen was born in Khulna, Bangladesh on September 08, 1975. He received his B.Sc. Eng. Degree from Rajshahi University of Engineering and Technology (RUET), Bangladesh in 2000 and M. Sc. Eng. and Dr. Eng. Degrees from Kitami Institute of Technology, Japan, in 2005 and 2008 respectively, all in Electrical and Electronic Engineering. Presently he is doing research works under the JSPS (Japan Society for the Promotion of Science) Postdoctoral Fellowship Program at the Kitami Institute of Technology, Japan. Dr. Muyeen is a member of the IEEE. His research interests are power system, electrical machine, FACTS, energy storage system (ESS), wind generator stabilization, and multi-mass drive train of wind turbine.

Rion Takahashi received the B.Sc. Eng. and Dr. Eng. Degrees from Kitami Institute of Technology, Japan, in 1998 and 2006 respectively, all in Electrical and Electronic Engineering. Now he is working as research assistant in Department of Electrical and Electronic Engineering, Kitami Institute of Technology. His major research interests include analysis of power system transient, FACTS and wind energy conversion system.

Toshiaki Murata completed his Electrical Engineering Curriculum of the Teacher Training School from Hokkaido University, Japan. Since 1969, he had been a Research Assistant at the Kitami Institute of Technology, Japan. He received Dr. Eng. degree from Hokkaido University in 1991. Presently he is an associate professor at the Kitami Institute of Technology.

Junji Tamura received his B. Sc. Eng. Degree from Muroran Institute of Technology, Japan, in 1979 and M.Sc. Eng. and Dr. Eng. degrees from Hokkaido University, Japan, in 1981 and 1984 respectively, all in electrical engineering. In 1984, he became a lecturer and in 1986, an associate professor at the Kitami Institute of Technology, Japan. Currently he is a professor at the Kitami Institute of Technology. He is the senior member of IEEE.